HIGH-ACCURACY ATMOSPHERE CORRECTION FOR HYPERSPECTRAL DATA (HATCH)

Zheng Qu,[1] Alexander F. H. Goetz,[1,2] and Kathleen B. Heidebrecht[1]

1. INTRODUCTION

The ATmosphere REMoval program (ATREM, Gao, *et al*., 1993) has been widely used in the hyperspectral remote sensing community for over 10 years. It works fast and delivers surface reflectance retrieval with reasonable accuracy. Yet the major techniques employed in ATREM are now outdated as a result of new advancement in the area of atmospheric radiative transfer. These include

1) the Malkmus band model based on HITRAN 92 database: HITRAN 96 and HITRAN 99 are now available with more accurate molecular line parameters. Also ATREM employs the multiplication rule to handle transmittance in spectral regions where multiple gas absorption is present. This results in less accurate transmittance calculation in these regions, *e.g.*, at $2.0\mu m$ where both H2O and CO2 strongly absorb.
2) separation of multiple scattering process from absorption process in the atmosphere: this is a result from the use of a band model for gaseous transmittance calculation. It causes less accurate path radiance calculation for short wavelengths and for turbid atmospheric conditions.
3) the three-band ratioing technique for water vapor amount retrieval: the prerequisite for this technique is that the surface reflectance spectrum is linear in wavelength in the water vapor absorption region to be used. This brings about retrieval errors when the surface reflectance spectrum is not linear for wavelength, for instance, for iron rich soil and wet vegetation.

In this paper we report our progress in the development of the HATCH (Height-accuracy ATmospheric Correction for Hyperspectral Data) program. HATCH aims at retrieving surface reflectance spectra of high quality with reasonable speed. The improved performance over ATREM will be a result mostly from implementation of state-of-the-art techniques in the area of atmospheric radiative transfer.

Since HATCH specifically targets at the atmospheric radiative transfer problems in visible and SW IR regions only, in order to speed up the data processing, we use our own radiative transfer algorithm rather than the general purpose atmospheric transmission code MODTRAN (Berk *et al*., 1989).

2. CORRELATED-*K* METHOD FOR GASEOUS ABSORPTION

The correlated-*k* method (Lacis and Oinas, 1991; Goody *et al.*, 1989) for gaseous absorption calculation transforms the line-by-line integration over a narrow spectral band of a radiative quantity, *e.g.* transmittance, to integration over the cumulative probability distribution function of the gas absorption coefficient. The transformed integration can therefore be computed using a few quadrature points without compromising accuracy, since the function to be integrated is a smooth one.

The correlated-*k* data in HATCH is generated by the line-by-line code LBLRTM (Clough and Iacono, 1995) based on HITRAN 96 database (Rothman, 1996). The data is independent of the algorithm and is easy to update once the new version of HITRAN database is available. Different data sets are generated for various possible gas mixing ratios for the overlapping absorption spectral regions.

Besides a better accuracy for computing gas absorption, the correlated-*k* method also provides an explicit way to accurately account for the interaction between multiple scattering and absorption. Multiple scattering increases the effective path length of a photon, and consequently increases the probability of a photon getting absorbed during transmition. A more accurate account for this interaction by using correlated-*k* method is thus expected to improve HATCH performance in the short wavelength regions.

[1] Center for the Study of Earth from Space/CIRES, University of Colorado, Boulder, CO 80309
[2] Department of Geological Sciences, University of Colorado, Boulder, CO 80309

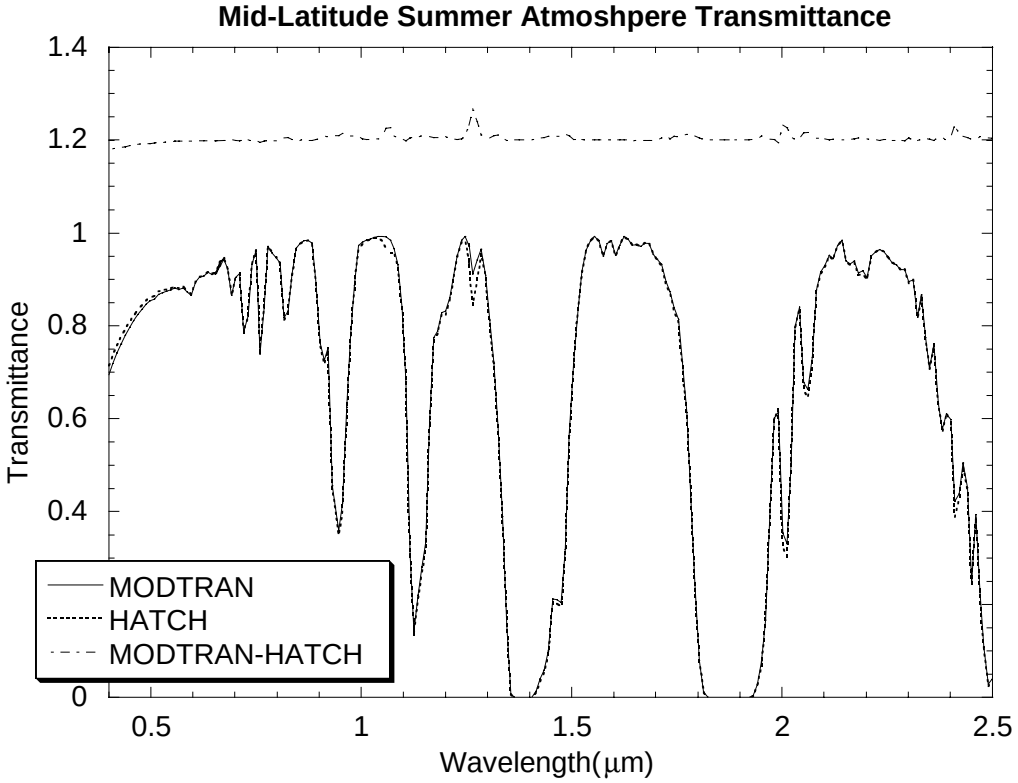

Figure 1. Mid-latitude summer atmosphere transmittance computed from HATCH and MODTRAN4. The results are convolved to AVIRIS band widths.

Figure 1 gives a comparison of transmittance computed from MODTRAN4 and from HATCH for a standard mid-latitude summer atmosphere with an overhead illumination. The major difference of the two transmittances lies in the 1.27 O_2 continuum region. Use of the recently published HITRAN99 database might bring down the difference. Other noticeable regions are 2.0μm overlapping region by water vapor and CO_2 as well as 2.3μm region where water vapor and CH_4 absorption overlaps. The possible explanation may come from the different ways in treating the overlapping absorption in the two models.

3. RT SOLVER: MULTI-GRID DISCRETE ORDINATES METHOD

The at-sensor radiance L can be related to the Lambertian surface reflectance ρ by

$$L = L_a + \frac{T_2 \rho}{1 - s\rho} \frac{S_0 \cos\theta_0}{\pi} \qquad (1)$$

where
L_a: atmospheric path radiance; T_2: two way transmittance for the sun-surface-sensor path; s: spherical albedo of the atmosphere; S_0: exoatmospheric solar irradiance; θ_0: solar zenith angle.

The major computation task before HATCH does surface reflectance retrieval on a pixel by pixel basis is to compute the three radiative quantities L_a, T_2, and s for a given solar-sensor geometry and the tabulated water vapor amounts. In order to speed up the computation, we implemented a new method for solving the radiative transfer

equation, called Multi-Grid discrete ordinates Radiative Transfer (MGRT) method (Qu and Goetz, 1999). The new method delivers a comparable accuracy to DISORT (Stemnes *et al*., 1988), which is widely used in RT calculation, including MODTRAN4, and is 5-10 times faster in radiance calculation.

Basically the new method solves the integral form of the RT equation and employs the linearity of the equation to speed up the convergence of the iteration process by computing the residual on fewer streams. For example, it solves the equation on a two-stream grid to compute the residual from a four-stream iteration. It generally converges in less than 5 iteration cycles.

Table 1. The relative CPU time comparison for DISORT and HATCH .

	4-stream	8-stream	16-stream	24-stream
DISORT	1	3.5	18.8	69.2
MGRT	0.15 ~ 0.2	0.35 ~ 0.5	1.7 ~ 2.0	6.5 ~ 8.0

Table 1 presents the relative CPU time comparison for DISORT and HATCH when performing a radiance computation over the range 0.4-2.5μm at 1nm interval. Figure 2 gives accuracy comparisons between DISORT and HATCH for a mid-latitude summer atmosphere TOA upwelling radiance at μ = 0.9 and 1, and $\phi = 0^o$, 45^o, 90^o, 135^o and 180^o, where μ is the negative cosine viewing zenith angle and ϕ is the relative azimuth angle to solar beam incident plane. The solar zenith angle is at 45^o. Again the wavelength range is between 0.4 and 2.5μm. Results are plotted in ratios of RMS difference over mean between MGRT and DISORT, using DISORT 24-stream results as baselines. The MGRT convergence behavior is also shown in Figure 2 as curves denoted by "MGRT-MGRT (24 STR)", using MGRT 24-stream results as baselines. Note some differences shown here are due to different treatment of atmospheric layering. DISORT divides the atmosphere into a number of optically homogeneous layers while MGRT computes radiative quantities over a number of vertical grid points and assumes that the optical properties vary linearly across adjacent grid points.

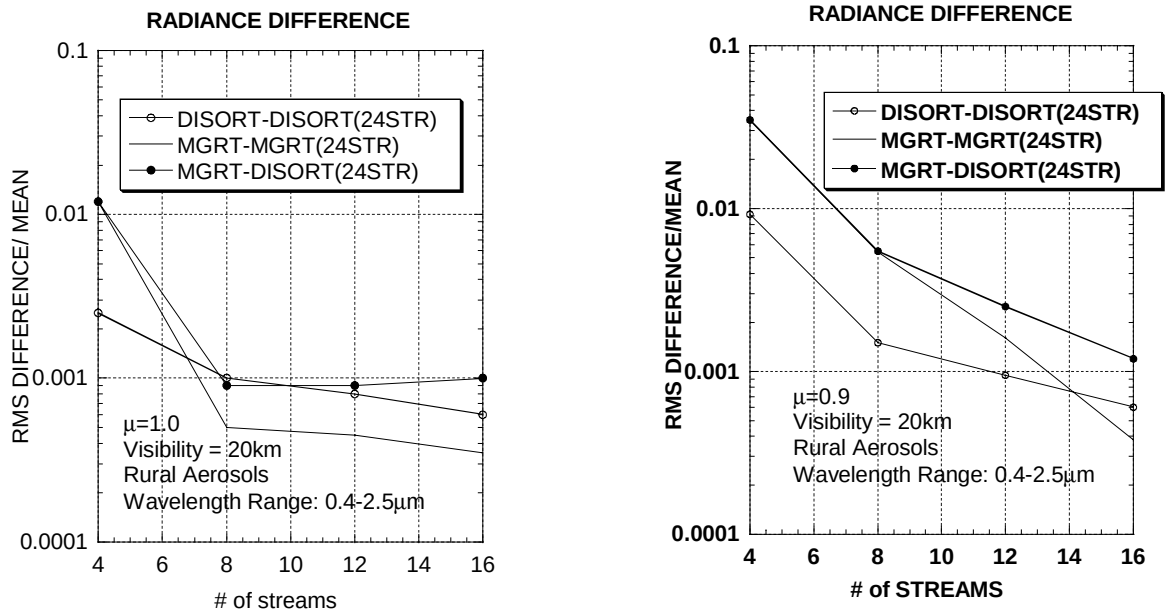

Figure 2. Relative accuracy for upwelling radiance computed from MGRT as compared to DISORT.

4. WATER VAPOR AMOUNT RETRIEVAL

Water vapor amount is one of the major uncertain factors in the atmospheric components that affect radiation in the 0.4-2.5μm spectral regions. Gao *et al*. (1993) proposed the three-band ratioing technique for water vapor amount retrieval which requires the surface reflectance values at the selected three channels to be linear in wavelength. The three- band ratioing technique works fairly well for most surface types. Yet systematic errors are introduced for vegetation surfaces, snow/ice surfaces, and iron-rich soils.

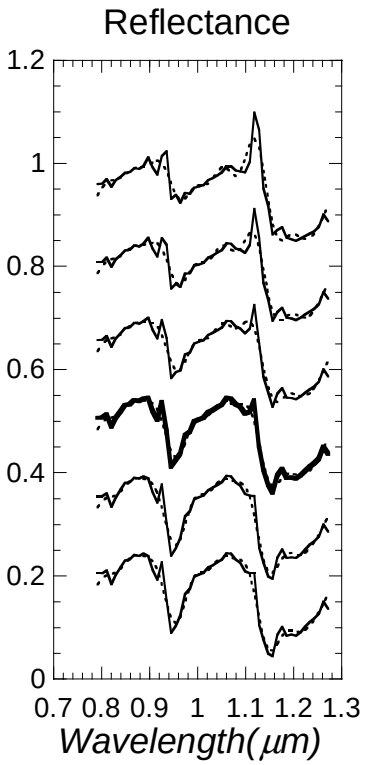

Figure 3. "Smoothness test" for water vapor retrieval. Adjacent reflectance spectra offset: 0.15

The new technique, called "smoothness test", proposed here attempts to avoid the linearity assumption for the surface reflectance. It is based on the principle often used by hyperspectral data analysis researchers that either under- or overestimation of water vapor amount results in irregularities in the retrieved surface reflectance. Features generated from poor atmospheric corrections are generally rougher than the inherent surface spectral features. In other words, atmospheric transmission features contain more high frequency components than surface ones.

Therefore, the best water vapor estimation yields the smoothest retrieved surface reflectance in the water vapor absorbing regions. There are quite a few criteria that can be used for a smoothness test. Our criterion is as follows. First, surface reflectance in the .8-1.25μm spectral region is derived for a given amount of water vapor. Then a smoothed reflectance spectrum is constructed accordingly using a truncated Fourier series. The RMS difference between the two spectra serves as the smoothness criterion. The lower the RMS value, the smoother the spectrum.

Figure 3 shows the retrieved reflectance spectra using AVIRIS data and their corresponding smoothed ones. The fourth pair of spectra (thick solid line) from top corresponds to the proper water vapor amount derived by this technique.

Once the water vapor amount at the first pixel is derived, the next adjacent pixel can use this value as an initial guess and the smoothness test needs to be done only for a few different water vapor amounts to find the proper value.

5. AEROSOLS AND OTHER GASES

HATCH uses AFGL standard aerosol data (Shettle and Fenn, 1976) for tropospheric aerosols. One innovative function in HATCH is to allow different aerosol types to be mixed externally, *e.g*., a mixture of oceanic and urban aerosols can be used for coastal regions. Hence more accurate accounting of path radiance for short wavelength region can be achieved. The user will specify the aerosol loading and the mixing ratio. In future, these will be derived from instantaneous sunphotometer measurement or from the AVIRIS data itself.

Apart from water vapor, HATCH also determines amounts of other absorbing gases, such as carbon dioxide and methane. The smoothness test is again used for these procedures. However, unlike water vapor, these gaseous amounts are derived once per scene, since the spatial distribution of these gases does not vary as significantly as water vapor. This portion of the algorithm is still under development.

6. SPECTRAL CALIBRATION EXPERIMENT

Even after the water vapor amount is fine-tuned by the smoothness test, the derived AVIRIS reflectance spectra often show systematic spectral features in the water vapor absorption regions. These are suspected to be results from wavelength shifting during the flight. We performed a simple experiment. By shifting the center wavelength of the

spectrometer B, C, and D we acquired three sets of spectra in these regions. The smoothest spectrum, judged by the same criterion used for water vapor retrieval, may be associated with the proper wavelength shift.

Our preliminary experiment finds that the spectral shift determined this way is independent of water vapor amount and pixel location. The data we used for this experiment is a 1999 AVIRIS over flight at Boulder, CO. Figure 4 gives the radiance RGB image of the data. At site A (soil surface) a simultaneous surface reflectance measurement was taken at time of AVIRIS overflight. Reflectance spectra retrieved by ATREM and HATCH are plotted together with the surface measurement in Figure 5 with a 15% reflectance shifting for clarity. Improvement in reflectance values calculated by HATCH over ATREM at the wings of the strong absorption regions around 1.38μm, 1.9μm and 2.5μm is apparent to notice. This is primarily attributable to the use of correlated-*k* method and the new HITRAN database that more accurately accounts for gaseous absorption.

Figure 4. 09-30-1999 AVIRIS overflight at Boulder, CO.

Figure 5 also gives spectrally shifted HATCH spectrum described above, which is much smoother and matches the surface measurement better. At vegetation site B, surface reflectance spectra derived from ATREM and HATCH are plotted in Figure 6. Using the same spectral calibration method, we acquired the same spectral shifting values for spectrometer B, C, and D as in site A. The spectrally calibrated HATCH spectrum, which apparently contains much fewer atmospheric residual features than that without spectral calibration, is also plotted in Figure 6.

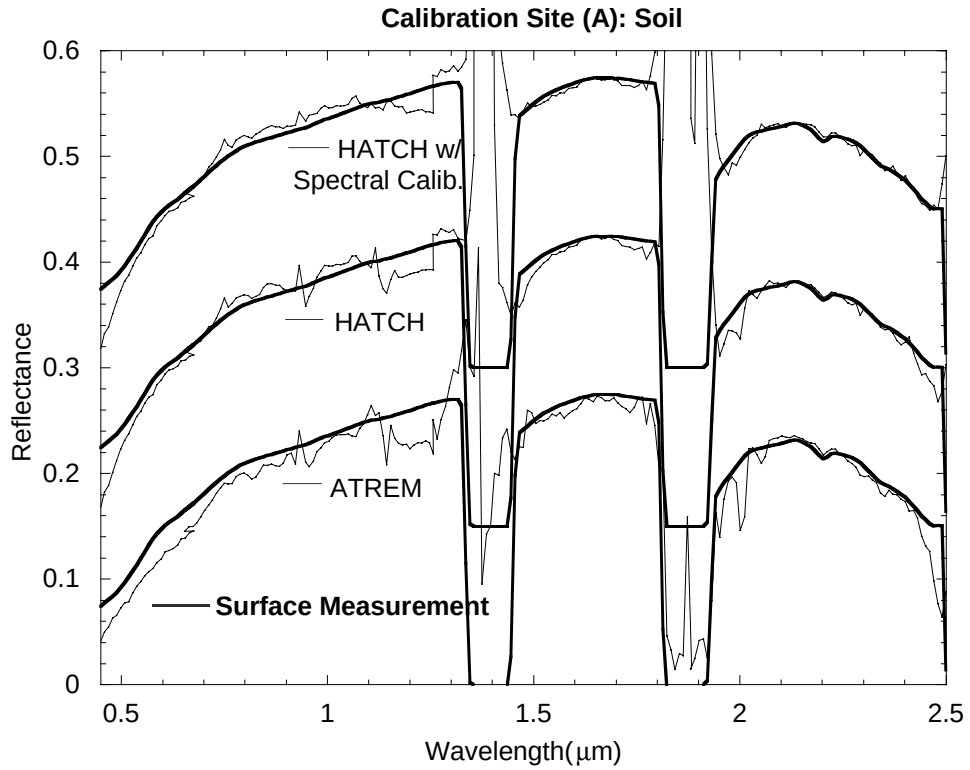

Figure 5. HATCH and ATREM derived as well as ASD measured surface reflectance for soil at

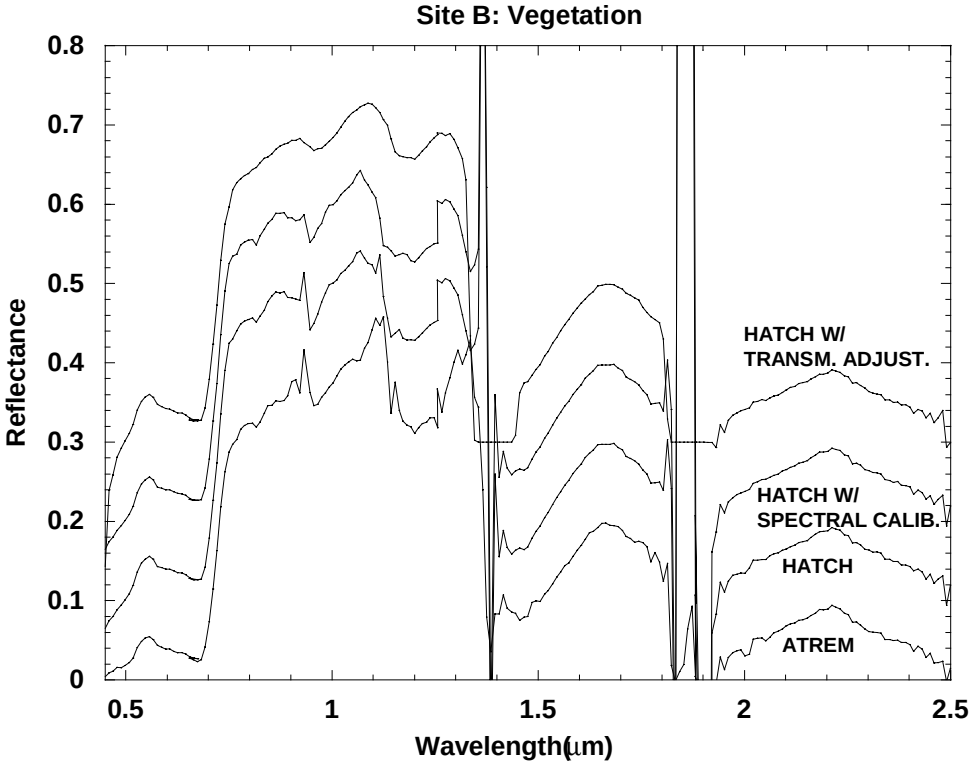

Figure 6. HATCH and ATREM derived surface reflectance for vegetation in site B.

7. POSTERIOR POLISHING

HATCH derived reflectance spectra, though improved over ATREM, still contain many systematic errors. Using a similar technique as used in empirical line method (Conel *et al.*, 1987), we use the surface measurement to obtain an adjustment spectrum for the two-way transmittance from site A and apply this transmittance adjustment to all other pixels to smooth out possible systematic errors. First, the two-way transmittance spectrum T_2^* is derived from the surface reflectance measurement ρ^* and the at-sensor radiance L^*, using equation (1):

$$T_2^* = (L^* - L_a)\frac{1 - s\rho^*}{\rho^*}\frac{\pi}{S_0 \cos\theta_0}$$

The transmittance adjustment spectrum is then computed as

$$\beta = \frac{T_2^*}{T_2}$$

where T_2 is the HATCH two-way transmittance associated with the HATCH derived water vapor amount at site A. The transmittance adjustment spectrum β is then applied to the two-way transmittance for all other pixels:

$$\rho = \frac{1}{s + \frac{T_2\beta}{L - L_a}\frac{S_0 \cos\theta_0}{\pi}}.$$

Unlike the empirical line method, adjustment here is applied for transmittance instead of surface reflectance, since we believe most of the errors are associated with atmospheric transmittance. This process lumps errors of all origins; uncertainties in atmospheric radiation properties, the exoatmospheric solar irradiance, calibration errors in the instrument, *etc.*, into the two-way transmittance. Figure 6 shows the reflectance spectrum for the vegetation in site B derived with HATCH using adjusted two-way transmittance. The resulting spectrum is the most realistic-appearing of the four plotted.

The posterior polishing process in future will also work without having to resort to surface measurement. The systematic transmittance adjustment spectrum will be derived from the data itself using the method presented by Goetz *et al.* (1997).

8. SUMMARY

With implementation of recent advancements in atmospheric radiative transfer, HATCH algorithm shows improvements in many aspects over ATREM. These include better performance around strong water vapor absorption regions and overlapping regions for different gases. The automatic spectral calibration capability has proved to be a promising function for HATCH to handle the problematic residual atmospheric feature in derived reflectance.

The major differences between HATCH and ATREM algorithm are listed in Table 2.

Table 2. Comparison between HATCH and ATREM algorithms.

	HATCH	**ATREM**
Gaseous Absorption	Correlated-k (Hitran96)	Malkmus Band Model (Hitran92)
RT Solver	Multi-Grid Discrete Ordinate Method	Successive Order Approach (6S)
H2O Retrieval	Smoothness Test	3-band Ratioing
CO2, CH4 Retrieval	Smoothness Test	
Different Aerosols Types	Can Be Mixed Externally	
Posterior Polishing	Spectral Calibration & Transmittance Adjustment	

9. ACKNOWLEDGEMENTS

This research was carried out under contracts NAG5-4447 and NCC5-458 from the National Aeronautics and Space Administration.

10. REFERENCES

Berk, A., L.S. Bernstein, and D.C. Robertson (1989), MODTRAN: A moderate resolution model for LOWTRAN 7, Final report, ***GL-TR-0122***, AGFL, Hanscom AFB, MA, 42 pp.

Clough, S.A., and M.J. Iacono (1995), Line-by-line calculation of atmospheric fluxes and cooling rates. application to carbon-dioxide, ozone, methane, nitrous-oxide and the halocarbons, *J. Geophys. Res.*, ***100,*** *D8:* 16519-16535.

Conel, J.E., R.O. Green, G. Vane, C.J. Bruegge, R.E. Alley, and B. Curtiss (1987), Airborne Imaging Spectrometer-2: Radiometric spectral characteristics and comparison of ways to compensate for the atmosphere, *Proc. SPIE*, **834**: pp. 140-157.

Gao, B.-C., K.B. Heidebrecht, and A.F.H. Goetz (1993), Derivation of scaled surface reflectance from AVIRIS data, *Remote Sens. Environ*., ***44***: pp. 165-178

Goetz, A.F.H., J. Boardman, B. Kindel, and K.B. Heidebrecht (1997), Atmospheric corrections: On deriving surface reflectance from hyperspectral imagers, *Pro. SPIE*, **3118**: pp.14-22.

Goody, R., R. West, L. Chen, and D. Crisp (1989), The correlated-*k* method for radiation calculations in nonhomogeneous atmospheres. *J. Quant. Spectrosc. Radiat. Transfer*, ***42***: 539-550.

Lacis, A.A., and V. Oinas (1991), A description of correlated *k* distribution method for modeling nongray gaseous absorption, thermal emission, and multiple scattering in vertically inhomogeneous atmospheres. *J. Geophys. Res*. ***96***: 9027-9063.

Qu, Z., and A.H. Goetz (1999), A fast algorithm for radiative intensity calculation in plane parallel scattering-absorbing atmospheres, *22nd Annual Review of Atmospheric Transmission Models*, Hanscom AFB, MA (7-10 June 1999).

Rothman, L.S., C.P. Rinsland, A. Goldman, S.T. Massie, D.P. Edwards, J. -M. Flaud, A. Perrin, C. Camy-Peyret, V. Dana, J. -Y. Mandin, V. Nemtchinov, and P. Varanasi (1996), The 1996 HITRAN Molecular Spectroscopic Database and HAWKS (HITRAN Atmospheric Workstation), *J. Quant. Spec. Radiat. Transf*., ***60***, 5: 665-710.

Shettle, E.P., and R.W. Fenn (1976) Models of atmospheric aerosols and their optical properties. In *AGARD Conference Proceedings No. 183*, Optical Propagation in the Atmosphere. ***AGARD-CP-183*** (NTIS, ADA 028615).

Stamnes, K., S.-C. Tsay, W. Wiscombe and K. Jayaweera, 1988: A numerically stable algorithm for discrete-ordinate-method radiative transfer in multiple scattering and emitting layered media, *Appl. Opt*. ***27***: 2502-2509.